

A Computational adsorption and DFT studies on corrosion inhibition potential of some derivatives of phenyl-UREA

David Ebuka Arthur, Adamu Uzairu, Abdullahi Mustapha and Elijah Shola Adeniji

Department of Chemistry, Ahmadu Bello University Zaria. Nigeria

Received November 22, 2018; Accepted January 16, 2019; Published January 22, 2019

Copyright: © 2019 Ebuka A. David.

***Corresponding author:** Ebuka A. David, Department of Chemistry, Ahmadu Bello University Zaria. Nigeria, Email: eadavid@abu.edu.ng

Abstract

Trends of inhibiting corrosion by HU1 and HU2 were explored with the use of the theory of density functional (DFT) at the B3LYP/6-311 + G(d,p) level of theory. The quantum chemical descriptors calculated for the two compounds or chemical parameters were correlated with its corrosion inhibition efficiency. The molecular descriptors have been analyzed through the function of Fukui and soft local indices, to compare the possible sites of electrophilic and Nucleophilic attack. The success of the calculation of the DFT in the prediction of the efficacy of inhibition is reported to be satisfactory, and the result reveals that HU2 with the energy of adsorption of -91.38 is greater than the HU1, that is -394.42 kJ/mol. The deformation energy of the inhibitor HU1 and HU2 was reported as -307.11 and 8.05 kJ/mol respectively, suggesting that the interaction between HU2 and the metal surface is more stable and would require an additional energy to dissociate their interaction.

Keywords: Iron; Adsorption; Corrosion; DFT method; Fukui Function; phenyl-urea.

Introduction

Corrosion of metals is possibly the problem more insistent in the industries of today, a problem that has rapt many researchers and scientists from around the world. The safety of metal against corrosive surfaces is a vital scientific topic as noted above by numerous authors [1–3].

Corrosion may also be considered as a redox process in which an oxide coating is formed on the surface of the metal/alloy undergoing the process. It therefore requires oxygen and moisture to occur. It involves the transfer of electrons along the surface of the metal under the influence of a potential difference. Most metals corrode on contact with water, acids, bases, oil and salts etc. The main reason for metals to corrode is their tendency to

return to their naturally occurring forms which is accompanied by a decrease in the free energy of the system.

Corrosion remains a major problem all around the world. And this could be controlled by application of corrosion resistant materials as well as by efficient corrosion inhibitors in different fields (cooling systems, oil and gas industry, paints etc.). The inhibitors reduces the corrosion of metals/alloys by application of its little concentration, acting either as a barrier by forming an adsorbed layer on the metal surface or retarding one of both electrochemical processes cathodic or anodic inhibitors. Despite availability of many metals (e.g. stainless steel, aluminum, etc.) that can be used in various industrial applications, iron or low carbon steels are still the most widely used engineering materials. Because of their low cost and mechanical properties, carbon and low-alloy steels are the workhorse materials in most industries. This includes the oil and gas industry, where these materials remain the most used materials for structural members, plates, sheets, tubing and flow lines and transmission pipelines.

Compounds composed of lone pairs of electrons are greatly useful in preventing corrosion of metals. For example, some researchers

said the effective inhibition of corrosion in steel and iron by organic compounds contain heteroatoms [3–8]

The corrosion inhibitors studied in the past revealed that the chemical nature involving properties like functional groups, electron density at the donor atom, p-orbital character, and the electronic structure of the molecule was mainly responsible for manipulating the adsorption of these inhibitors onto the metal surface [3,9–11].

Currently, computer modeling techniques have been used effectively for the study of corrosion of metals [12-15]. One method includes DFT which is used in the calculation of reactive properties such as functions of Fukui in revealing the orbitals used responsibly for interaction between the metal surface and the inhibitor [16].

Material and methods

The present calculations were performed using Spartan 14 V 1.1.4 (Wavefunction program package) [17].

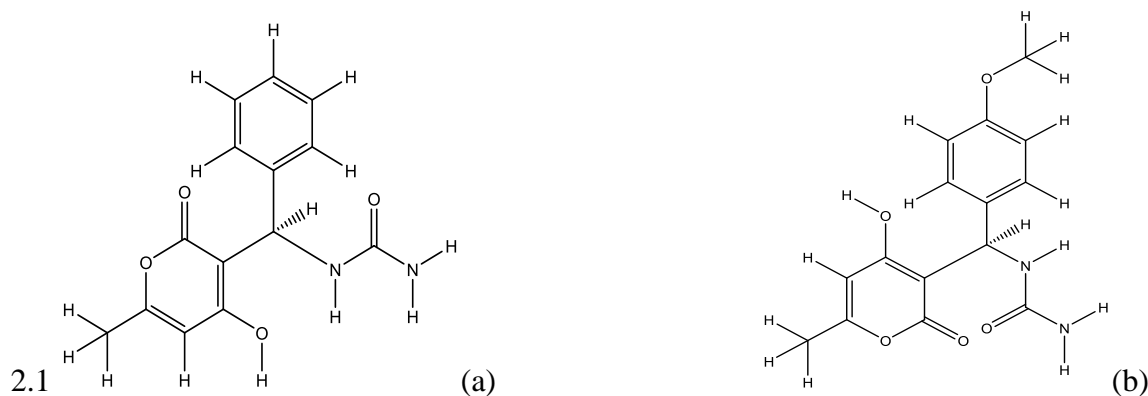


Figure 1: The molecular structures of the investigated inhibitors: (a) [(4-Hydroxy-6-methyl-2-oxo-2H-pyran-3-yl)-phenyl-methyl]-urea (HU1) (b) [(4-Hydroxy-6-methyl-2-oxo-2H-pyran-3-yl)-(4-methoxy-phenyl)-methyl]-urea (HU2)

Compound(M)	Rs (Ω.cm2)	Rct (KΩ.cm2)	C(μF.cm2)	IE%
Blank	3.230	1.790	63.020	-
HU1	1.400	6.007	94.300	70.200
HU2	1.030	8.960	159.000	80.000

Table 1: Impedance parameters for stainless steel type 316 in phosphoric acid in presence of inhibitors HU2 and HU1

The organic inhibitors used in this research work, namely [(4-Hydroxy-6-methyl-2-oxo-2H-pyran-3-yl)-phenyl-methyl]-urea (HU1) and [(4-Hydroxy-6-methyl-2-oxo-2H-pyran-3-yl)-(4-methoxy-phenyl)-methyl]-urea (HU2). Were reported by [2], as effective compounds as corrosion inhibitors, since their inhibition efficiency was good, following their result which is explicitly shown in Table 1. This reference helps justify which of these compounds freely would prevent corrosion of steel by means of adsorption. Where the parameters in Table 1 is defined as E% = inhibition efficiency, Rs = solution resistance, Rct = charge transfer resistance and C = double layer capacitance.

Geometry optimizations were carried-out using DFT [18], which take in a mixture of HF with DFT exchange terms associated with the gradient-corrected correlation functional of Lee, Yang, and Parr (LYP) [16] and the 6-311 + G(d,p) basis set. In the geometry optimizations process, constraints on the chemical structures were removed from end to end using molecular mechanics process. Frontier molecular orbitals such as lowest unoccupied molecular orbital (LUMO) and highest occupied molecular orbital (HOMO) was used to show the point of adsorption of the inhibitors on top of the metal surface. According to Koopman's theorem, the energies of the HOMO and LUMO orbitals are associated with the ionization potential and electron affinity correspondingly (equation 1&2):

$$I = -E_{\text{Homo}} \quad \text{----- (1)}$$

$$A = -E_{\text{Lomo}} \quad \text{----- (2)}$$

Electronegativity (χ), and hardness (η), of the inhibitor molecule, are specified in equation 3&4

$$\chi = (I + A) / 2 \quad \text{----- (3)}$$

$$\eta = (I - A) / 2 \quad \text{----- (4)}$$

The softness is the inverse of the hardness (equation 5)

$$\sigma = 1 / \eta \quad \text{----- (5)}$$

The significance of evaluating electronegativity, hardness, and softness in corrosion chemistry was reported, in proficiently studying chemical reactivity regarding metal interaction with other chemical specie. The interaction of Fe and inhibitor proposes that electrons will run from lower χ (inhibitor) to higher χ (Fe), up until the chemical potentials come to be the same.

The volume of conveyed electrons (ΔN), was calculated with the equation

$$\Delta N = (\chi_{\text{Fe}} - \chi_{\text{inh}}) / 2(\eta_{\text{Fe}} + \eta_{\text{inh}}) \quad \text{----- (6)}$$

η_{Fe} and η_{inh} in equation (6) symbolize the absolute electronegativity of iron and inhibitor molecule distinctly, while χ_{Fe} and χ_{inh} represents the absolute hardness of iron and inhibitor molecule, respectively.

The global electrophilicity index presented by Parr [19, 20] is given as

$$\omega = \mu^2/2\eta \quad \text{-----} \quad (7)$$

Affording to the report, this index measures the propensity of chemical species to accept electrons. A good nucleophile is identified by the lower value of χ and ω (equation 7). This new reactivity index measures the balance of energy when there are an extra electronic charge ΔN rolling from the surroundings into the system.

The aim of this paper is to determine the relationship between quantum chemical descriptors and the experimental inhibition

efficiencies of the inhibitors, by measuring the quantum chemical parameters to justify the behaviors of the inhibitors with an iron surface.

Results and Discussion

Figure 2 shows the optimized structures of HU1 and HU2 inhibitors with a systematic atomic numbering, while Figure 3 shows the LUMO and HOMO or frontier orbitals of the inhibitors. The computed quantum chemical properties such as EHOMO, ELUMO, ΔE_{L-H} and dipole moment of the inhibitors (HU1 and HU2) optimized are presented in Table 2.

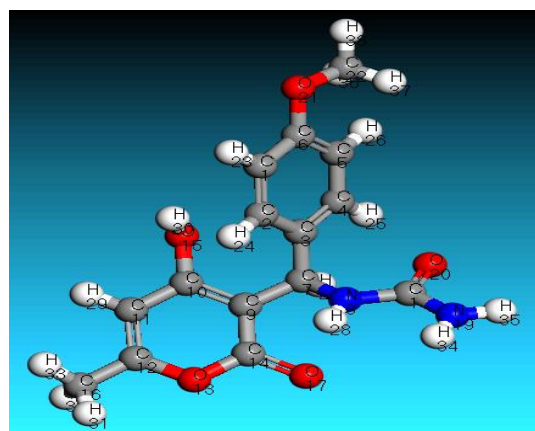
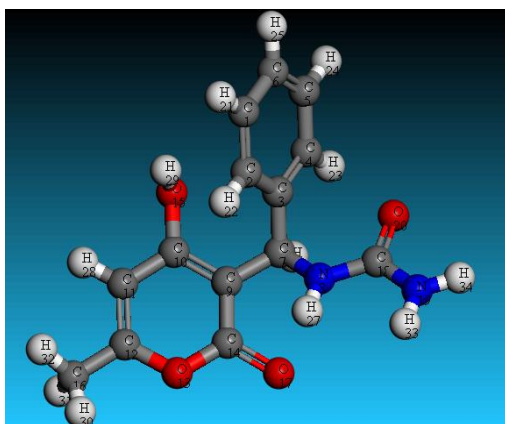


Figure 2: Optimized geometries of (a) [(4Hydroxy6methyl2oxo2Hpyran3yl) phenylmethyl] urea (HU1) (b) [(4Hydroxy6methyl2oxo2Hpyran3yl) (4methoxyphenyl)methyl]urea(HU2) molecules along with atomic numbering calculated at B3LYP/6-31 + G(d, p) level of theory

Quantum parameters	HU1	HU2
E_{Homo} (eV)	-5.96	-5.66
E_{Lumo} (eV)	-1.01	-0.96
ΔE_{L-H} (eV)	4.95	4.70
μ (debye)	1.82	1.03

Table 2: Calculated quantum chemical properties for the most stable conformation of the HU1 and HU2 molecules calculated at B3LYP/6-31 + G (d,p) level of theory.

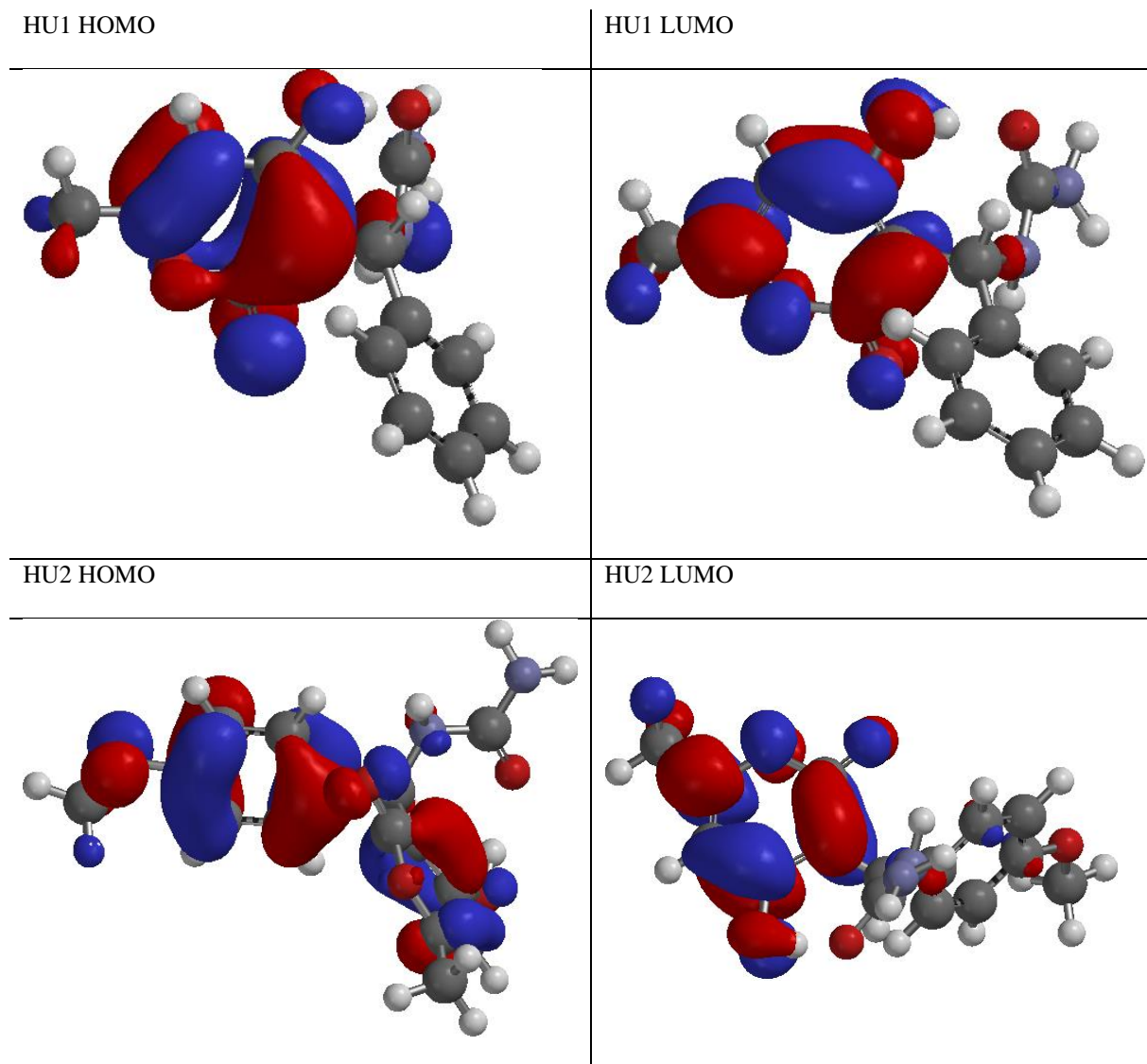


Figure 3: Frontier molecular orbitals (FMO) of HU1 and HU2 molecules calculated at B3LYP/6-31 + G(d,p) level of theory, the colour red represent nucleophilic parts of the compound while the blue colour symbolises electrophilic part.

In the chemistry of corrosion process, inhibition of metal corrosion starts with contact, between the frontier molecular orbitals of the metal exterior and the inhibitor. where the electrons on the metal surface is placed on the LUMO of the inhibitor and

the lone pair electrons or in anions the charged surface donates the bonding electron into the d-orbital of the metal [21,22]. The LUMO energy of HU2 (-0.96 eV) is less negative than that of HU1 which is -1.01 and because of the excess electron on the

metal surface with the HU2 inhibitor, the LUMO of HU2 will readily accept some of the excess electron from the surface of the metal thereby making HU2 molecule more likely for interaction.

The energy gap is an additional parameter essential in elucidating DFT studied reactions, it aids as a role of reactivity of the inhibitor molecule to the adsorption on the metal surface [23]. Energy gap defines the stability of a chemical specie in a chemical environment [16]. HU2 inhibitor has the lowest energy gap (4.70 eV) when compared to HU1 inhibitor (4.95 eV) which can be seen in Table 2. The variance in their energy gap is roughly equal to 0.25 eV which is sufficient to create a change in the system this means that HU2 molecule may perhaps have improved performance as carrion inhibitor than HU1 molecule, a conclusion that completely agrees with the experimental finding [2].

The dipole moment (μ) for HU1 and HU2 calculated, is an electronic parameter that defines the degree of charge circulation around the surface of the molecule, it can be used to forecast the reactivity and firmness of molecules [24]. The high value of dipole moment leads to an increase in deformation energy, making the adsorbed molecule at the ferrous surface rather unstable and unsuitable as a corrosion inhibitor [25–27].

In Table 2, the dipole moment of HU2 (1.03 Debye) supports the experimental result, which claims HU2 is a better inhibitor when compared to 1.82 Debye of HU1 [30] Other computed quantum chemical properties such as ionization energy, electron affinity, absolute electronegativity, absolute hardness, absolute softness, absolute electrophilicity, the fraction of electron transferred, and the total energy for HU1 and HU2 inhibitors are reported in Table 3.

Quantum parameters	HU1(au)	HU2 (au)	Fe (au)
$I = -E_{\text{Homo}}$	0.219	0.208	0.197
$A = -E_{\text{Lumo}}$	0.037	0.035	0.143
$\chi = \frac{I + A}{2}$	0.128	0.122	0.170
$\eta = \frac{I - A}{2}$	0.091	0.086	0.027
$\sigma = \frac{1}{\eta}$	11.008 au ⁻¹	11.607 au ⁻¹	37.037 au ⁻¹
$\omega = \frac{\mu^2}{2\eta}$	43.883	13.350	
$\Delta N = \frac{\chi_{\text{fe}} - \chi_{\text{inh}}}{2(\eta_{\text{fe}} + \eta_{\text{inh}})}$	20.174	18.553	
E_{tot}	-952.351	-1066.873	

Table 3: Calculated quantum chemical parameters of HU1 and HU1 molecules calculated at B3LYP/6-31 + G (d,p) level of theory in atomic units

Ionization energy (I) and electronegativity (χ) are important molecular descriptors to be considered when studying chemical reactions involving inorganic species like metals and molecules, they were calculated for HU1 and HU2 and reported in Table 3. High ionization energy indicates high stability and chemical inertness while high electronegativity is the opposite [28]. The high ionization energy of HU2 (0.208 au) and Low electronegativity (0.035 au) supports its high inhibition efficiency than when compared to HU1 whose ionization energy and electronegativity given as 0.219 au and 0.037 au respectively clearly indicates that HU2 will readily react with the metal surface than HU1.

Absolute hardness (η) and softness (σ) of HU1 and HU2 were also calculated and reported in Table 3 reflects on the measure of molecular stability and reactivity of the inhibitors. A hard molecule has a large energy gap and a soft molecule has a small energy gap [23]. In this study HU2 with low hardness value $\eta = 0.086$ au. Compared to that of the HU1 $\eta = 0.091$ au. The absolute softness was found to be higher in HU2 (11.607 au) than HU1 (11.008 au) which supports the experimental result since the inhibition efficiency is higher in HU2 than in HU1 [2].

The number of electrons transferred (ΔN) was also calculated and tabulated in Table 3. If $\Delta N < 3.6$, the inhibition efficiency

increases and in return increasing the electron-donating ability of these metals to donate electron to the metal surface [9] and the results indicate that ΔN values for the inhibitors HU1 and HU2 supports the experimental inhibition efficiencies.

The total energy of HU2 inhibitor is $E_{\text{tot}} = -1066.873$ au, while for HU1 inhibitor it is $E_{\text{tot}} = -952.351$ au, this tends to support the argument on which inhibitor active centers would favour adsorption process on the metal surface. From the result stated in Table 3, HU2 would adsorb more and prevent corrosion of the mild steel more than HU1, this agrees well with the experimental inhibition efficiency reported by Hnini.

Computational Adsorption Study

The simulations were realized by means of the DFT electronic structure programme DMol3 using a Fukui function and orbital analysis [29]. Electronic parameters for the model contain constrained spin polarization by means of the DND basis set and the Perdew–Wang (PW) local correlation density functional. Non-covalent adsorption of the molecules on the Fe surface was explored at a molecular level by molecular dynamics (MD) simulations, which was attained by Forcite quench molecular dynamics in the Material Studio software to mock-up diverse low energy conformations and recognize the truncated energy minima [12,30].

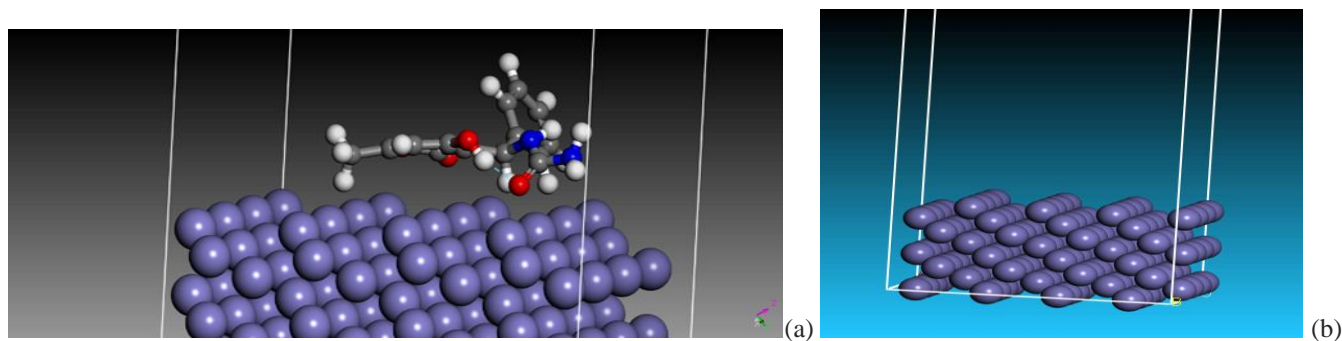


Figure 4: A diagram of Fe surface and adsorption of HU1 on the Fe surface shown in B

Figure 4 shows the energy of HOMO and LUMO of the optimized adsorption structures for single molecules of HU1 and HU2 on the Fe (110) surface. From our simulations, the molecules can be seen to orient on the Fe surface using the frontier orbitals as shown in Figure 4B, the simulation as expected shows the Atom (O20) pointing directly towards the surface of the metal, this was supported by the result of the Fukui indices for electrophilic attack in which the atom has the highest value i. e ($f_- = 0.208$).

The Adsorption isotherm provides important theoretical information necessary for this study. The evaluation of adsorption

isotherms for a mixture of adsorbates in an adsorbent framework on a sequence of fixed pressure models at a different temperature. For the duration of the recreation, molecules within the framework are erratically exchanged and, in addition, adsorbates are unsystematically generated in the framework. The configuration that results from these steps is accepted or rejected affording to the selection rules of the Monte Carlo method used. The total energy involved in the sorption process, the adsorption energy and deformation energy where calculated and reported for HU1 and HU2 in Table 4 and 6 respectively.

Total energy (kJ/mol)	Adsorption energy (kJ/mol)	Rigid adsorption energy (kJ/mol)	Deformation energy (kJ/mol)
-259.37	-394.42	-87.31	-307.11

Table 4: Calculated adsorption Parameters for HU1 adsorbent on the Fe (110) surface.

Fukui Indices for Electrophilic Attack (Fukui (f-))				Fukui Indices for Nucleophilic Attack (Fukui (f+))			
atom Mulliken Hirshfeld				atom Mulliken Hirshfeld			
C (1)	0.045	0.054		C (1)	0.010	0.009	
C (2)	0.026	0.033		C (2)	-0.017	-0.001	
C (3)	0.011	0.049		C (3)	-0.008	-0.004	
C (4)	0.026	0.050		C (4)	0.008	0.008	
C (5)	0.038	0.041		C (5)	0.009	0.011	
C (6)	0.057	0.071		C (6)	0.009	0.011	
C (7)	-0.010	0.006		C (7)	-0.005	0.009	
N (8)	0.025	0.033		N (8)	-0.013	0.000	
C (9)	0.001	0.001		C (9)	0.057	0.068	
C (10)	0.005	0.007		C (10)	0.108	0.108	

C (11)	0.010	0.010	C (11)	0.057	0.067
C (12)	0.010	0.012	C (12)	0.104	0.106
O (13)	0.009	0.010	O (13)	0.080	0.088
C (14)	0.012	0.008	C (14)	0.086	0.083
O (15)	0.014	0.023	O (15)	0.050	0.053
C (16)	0.000	0.004	C (16)	-0.004	0.029
O (17)	0.012	0.014	O (17)	0.122	0.114
C (18)	0.067	0.055	C (18)	0.011	0.009
N (19)	0.044	0.060	N (19)	0.007	0.009
O (20)	0.208	0.208	O (20)	0.014	0.014
H (21)	0.039	0.026	H (21)	0.009	0.006
H (22)	0.038	0.021	H (22)	0.012	0.005
H (23)	0.050	0.027	H (23)	0.010	0.006
H (24)	0.036	0.023	H (24)	0.009	0.006
H (25)	0.042	0.029	H (25)	0.008	0.006
H (26)	0.034	0.016	H (26)	0.034	0.019
H (27)	0.032	0.021	H (27)	0.014	0.009
H (28)	0.010	0.006	H (28)	0.057	0.036
H (29)	0.019	0.012	H (29)	0.033	0.029
H (30)	0.005	0.003	H (30)	0.037	0.024
H (31)	0.006	0.004	H (31)	0.047	0.034
H (32)	0.005	0.003	H (32)	0.034	0.023
H (33)	0.040	0.032	H (33)	0.005	0.004
H (34)	0.036	0.029	H (34)	0.006	0.005

Table 5: Fukui indices for nucleophilic and electrophilic attacks in HU1 calculated at LDA/PWC hybrid functional and DND basis set the level of theory

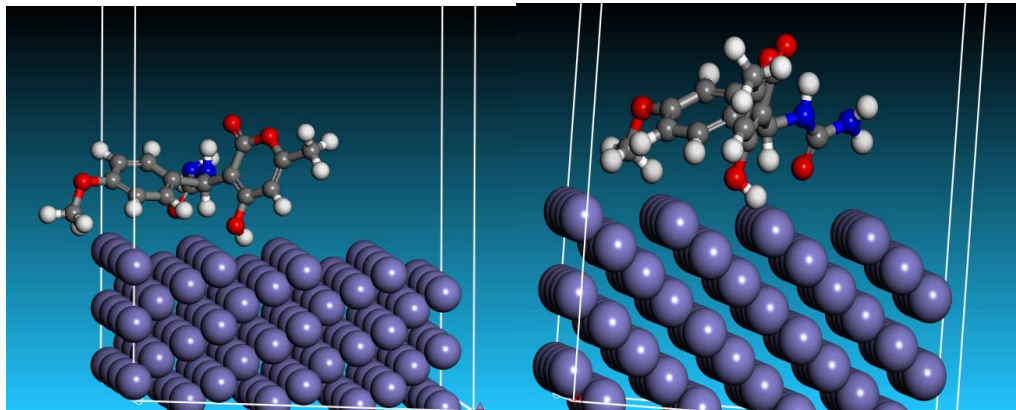


Figure 5: A sorption diagram of HU2 adsorbate on the Fe surface shown from different side view of the cleaved (110) plane.

Total energy (kJ/mol)	Adsorption energy (kJ/mol)	Rigid adsorption energy (kJ/mol)	Deformation energy (kJ/mol)
-269.62	-91.38	-99.43	8.05

Table 6: Calculated adsorption Parameters for HU2 adsorbent on the Fe (110) surface

The result of the adsorption parameters, which were calculated from the sorption study of HU1 and HU2 on cleaved Fe (110) surface, was shown in Figure 5 and reported in Table 4 and Table 6 respectively. The results show that the total energy required for the adsorption of HU2 (-269.62 kJ/mol) is lower than that of HU1 (-259.37), which indicates that the adsorption of HU2 on the Fe (110) cleaved surface is more likely than that of HU1. The firm

adsorption energy and deformation energy of HU2 also supports the adsorbates stability on Fe surface over HU1, additional emphasis may well be laid on the result of the Fukui indices for both compounds presented on Table 5 and 7, this result computationally explains why HU2 inhibits corrosion much more than HU1.

Fukui Indices for Electrophilic Attack (Fukui (f-))	Fukui Indices for Nucleophilic Attack (Fukui (f+))
---	--

atom	Mulliken	Hirshfeld	atom	Mulliken	Hirshfeld
C (1)	0.054	0.053	C (1)	0.011	0.009
C (2)	0.030	0.042	C (2)	-0.017	-0.002
C (3)	0.032	0.064	C (3)	-0.003	-0.003
C (4)	0.047	0.051	C (4)	0.008	0.008
C (5)	0.053	0.058	C (5)	0.008	0.009
C (6)	0.053	0.068	C (6)	0.007	0.008
C (7)	-0.006	0.008	C (7)	-0.008	0.008
N (8)	0.030	0.046	N (8)	-0.015	-0.001
C (9)	0.004	0.002	C (9)	0.060	0.069
C (10)	0.006	0.009	C (10)	0.107	0.108
C (11)	0.013	0.012	C (11)	0.056	0.067
C (12)	0.012	0.014	C (12)	0.105	0.107
O (13)	0.011	0.014	O (13)	0.079	0.088
C (14)	0.021	0.013	C (14)	0.085	0.082
O (15)	0.016	0.026	O (15)	0.048	0.052
C (16)	0.000	0.004	C (16)	-0.004	0.029
O (17)	0.032	0.036	O (17)	0.122	0.114
C (18)	0.028	0.028	C (18)	0.011	0.009
N (19)	0.038	0.042	N (19)	0.008	0.009
O (20)	0.063	0.062	O (20)	0.016	0.015
O (21)	0.075	0.075	O (21)	0.005	0.005
C (22)	-0.018	0.016	C (22)	-0.002	0.002
H (23)	0.043	0.028	H (23)	0.009	0.005

H (24) 0.042 0.023	H (24) 0.010 0.004
H (25) 0.044 0.026	H (25) 0.009 0.005
H (26) 0.041 0.026	H (26) 0.007 0.004
H (27) 0.033 0.015	H (27) 0.034 0.019
H (28) 0.033 0.021	H (28) 0.015 0.009
H (29) 0.011 0.007	H (29) 0.057 0.035
H (30) 0.021 0.013	H (30) 0.033 0.030
H (31) 0.006 0.004	H (31) 0.037 0.024
H (32) 0.007 0.005	H (32) 0.047 0.033
H (33) 0.006 0.004	H (33) 0.034 0.023
H (34) 0.021 0.018	H (34) 0.005 0.004
H (35) 0.022 0.019	H (35) 0.007 0.005
H (36) 0.026 0.016	H (36) 0.002 0.001
H (37) 0.029 0.017	H (37) 0.003 0.002
H (38) 0.023 0.014	H (38) 0.003 0.002

Table 7: Fukui indices for nucleophilic and electrophilic attacks in HU2 calculated at LDA/PWC hybrid functional and DND basis set the level of theory.

From the result of the DFT corrosion study and simulated molecular descriptors that support its experimental result of galvanized sorption study, the HU2 molecule is found to retain inhibition efficiency which is higher than that of HU1[2]. The

adsorption energy of HU2 is reported to be -91.38kJ/mol and that of HU1 is given as -394.42 kJ/mol, both adsorption energies supports a chemisorption process but favours the adsorption of HU2 more.

References

1. D.E. Arthur, A. Adedayo, G. Igelige, E. Ogwuche (2014) Corrosion Inhibition of Mild Steel in 0.1M H₂SO₄ Solution by Anacardium occidentale Gum 847–854.
2. K. Hnini, S. Fadel, M. Abderrahim, E.L. Mhammedi, A. Chtaini (2015) The Inhibition Effect of Heterocyclic Compounds towards the Corrosion of Iron in Phosphoric Media 1–13.
3. S.A. Umoren (2009) Polymers as Corrosion Inhibitors for Metals in Different Media - A Review 175–188.
4. P.O. Ameh, N.O. Eddy (2014) Characterization of Acacia Sieberiana (AS) Gum and Their Corrosion Inhibition Potentials for Zinc in Sulphuric Acid Medium 1 : 25–36.
5. M.A. Amin, S.S.A. Ei-rehim, E.E.F. El-sherbini, O.A. Hazzazi, M.N. Abbas (2009) Polyacrylic acid as a corrosion inhibitor for aluminium in weakly alkaline solutions . Part I: Weight loss , polarization , impedance EFM and EDX studies, Corros. Sci 51 : 658–667.
6. V.M. Abbasov, H.M.A. El-lateef, L.I. Aliyeva, E.E. Qasimov, I.T. Ismayilov et al. (2013) Applicability of Novel Anionic Surfactant as a Corrosion Inhibitor of Mild Steel and for Removing Thin Petroleum Films from Water Surface 1:18–23.
7. D.E. Arthur, C.E. Gimba, E.O. Nnabuk (2014) Miscibility Studies of Cashew Gum and Khaya Gum Exudates in Dilute Solution by Viscometry and FTIR Analysis 1–12.
8. E.E. Ebenso, M.M. Kabanda, T. Arslan, M. Saracoglu, F. Kandemirli (2012) Quantum Chemical Investigations on Quinoline Derivatives as Effective Corrosion Inhibitors for Mild Steel in Acidic Medium, Molecules 7 : 5643 – 5676.
9. N.A. Wazzan, F.M. Mahgoub (2014) DFT Calculations for Corrosion Inhibition of Ferrous Alloys by Pyrazolopyrimidine Derivatives 6–14.
10. M.M. Antonijevic, M.B. Petrovic (2008) Copper Corrosion Inhibitors . A review 3: 1–28.
11. D.E. Arthur, A. Jonathan, P.O. Ameh, C. Anya (2013) A review on the assessment of polymeric materials used as corrosion inhibitor of metals and alloys 1–9.
12. N. Boussalah, S. Ghalem, S. El Kadiri, B. Hammouti, R. Touzani (2013) Theoretical study of the corrosion inhibition of some bipyrazolic derivatives: a conceptual DFT investigation.
13. Z. El Adnani, A.T. Benjelloun, M. Benzakour, M. Mcharfi, M. Sfaira et al. (2014) DFT-based QSAR Study of Substituted Pyridine-Pyrazole Derivatives as Corrosion Inhibitors in Molar Hydrochloric Acid 9 : 4732–4746.
14. M. Ghiasi, S. Kamalinahad, M. Arabieh, M. Zahedi (2012) Carbonic anhydrase inhibitors: A quantum mechanical study of interaction between some antiepileptic drugs with active center of carbonic anhydrase enzyme, Comput. Theor. Chem. 992 : 59–69.
15. N.O. Eddy (2011) Experimental and theoretical studies on some amino acids and their potential activity as inhibitors for the corrosion of mild steel J. Adv. Res. 2 35–47.
16. W. Yang, R.G. Parr (1985) Hardness, softness, and the Fukui function in the electronic theory of metals and catalysis. Proc. Natl. Acad. Sci. U. S. A. 82 (1985) 6723–6726.

17. K.M. Manamela, L.C. Murulana, M.M. Kabanda, E.E. Ebenso (2014) Adsorptive and DFT Studies of Some Imidazolium Based Ionic Liquids as Corrosion Inhibitors for Zinc in Acidic Medium 3029–3046.
18. C. Lee, W. Yang, R.G. Parr (1988) Development of the Colle-Salvetti correlation-energy formula into a functional of the electron density, Phys. Rev. B. 37 (1988) 785–789.
19. Ponti, DFT-BASED CHEMICAL REACTIVITY INDICES.
20. M. Torrent-Sucarrat, F. De Proft, P.W. Ayers (2010) P. Geerlings, On the applicability of local softness and hardness., Phys. Chem. Chem. Phys 12 :1072–1080.
21. T. Joseph, H. Tresa, C.Y. Panicker, K. Viswanathan, M. Dolezal et al. (2013) Spectroscopic (FT-IR , FT-Raman), first order hyperpolarizability , NBO analysis , HOMO and LUMO analysis of N - [(4- (trifluoromethyl) phenyl) pyrazine- 2-carboxamide by density functional methods, Arab. J. Chem.
22. M.G. Elghalban, A.M. El Defarwy, R.K. Shah, M.A. Morsi (2014) α -Furil Dioxime : DFT Exploration and its Experimental Application to the Determination of Palladium by Square Wave Voltammetry 9: 2379–2396.
23. L.H. Mendoza-Huizar, C.H. Rios-Reyes (2011) Chemical reactivity of Atrazine employing the Fukui function, J. Mex. Chem. Soc. 55:142–147.
24. J.A. Seetula, R. June, A. October (1998) Kinetics of the $R + Cl$ ($R = CHCl$, $CHBrCl$, CCl and $CHCl$) reactions . An ab initio study of the transition states 3561–3567.
25. H.E. Gottlieb, V. Kotlyar, A. Nudelman (1997) NMR chemical shifts of common laboratory solvents as trace impurities, J. Org. Chem. 62 : 7512–7515.
26. S. Riahi, S. Eynollahi, S. Soleimani, M.R. Ganjali, P. Norouzi et al. (2009) Application of DFT method for determination of IR frequencies and electrochemical properties of 1,4-dihydroxy- 9,10- anthraquinone-2-sulphonate, Int. J. Electrochem. Sci 4 :1407–1418.
27. P.Udhayakala, T. V Rajendiran, S. Gunasekaran (2012) Theoretical Evaluation of Corrosion Inhibition Performance of Some Triazole Derivatives, Adv. Sci. Res 3 : 71–77.
28. A.K. Chandra, M.T. Nguyen (2012) Use of local softness for the interpretation of reaction mechanisms, Int. J. Mol. Sci 3 :310–323.
29. E.E. Oguzie, S.G. Wang, Y. Li, F.H. Wang, E.E. Oguzie (2009) Influence of Iron Microstructure on Corrosion Inhibitor Performance in Acidic Media Influence of Iron Microstructure on Corrosion Inhibitor Performance in Acidic Media.
30. E.E. Oguzie, C.E. Ogukwe, J.N. Ogbulie, F.C. Nwanebu, C.B. Adindu et al. (2012) Broad spectrum corrosion inhibition: corrosion and microbial (SRB) growth inhibiting effects 47 : 3592–3601.